Congruent Phase Transition at a Twist Boundary Induced by Solute Segregation

D. Udler and D. N. Seidman

Department of Materials Science and Engineering, Northwestern University, Evanston, Illinois 60208-3108

(Received 28 June 1995; revised manuscript received 22 July 1996)

A congruent or 2D structural phase transition is observed, via Monte Carlo simulations, in a $\Sigma = 5/(002)$ twist boundary that is induced by segregation of Ni from the bulk of a single-phase Pt(Ni) alloy bicrystal. This segregation induced phase transition, at 850 K, is from the coincident site lattice (CSL) structure to the type 2 structure, which involves a change in the space group from $p42_1'2'$ to $p42'2'$. For bulk concentrations up to 0.6 at. % Ni the boundary has the CSL structure, while for a bulk concentration of 7 at. % Ni the type 2 structure is stable. Evidence is presented for chemical ordering at this interface. [S0031-9007(96)01321-X]

PACS numbers: 68.35.Dv, 61.72.Mm

The existence of congruent or 2D phase transitions at grain boundaries (GBs) is now beyond any reasonable doubt [1]. In most cases the phase transitions are detected experimentally, while theoretical and simulational studies are lagging. One reason is that they occur at finite temperatures, and finite-temperature computational techniques—Monte Carlo (MC), molecular dynamics (MD), and lattice dynamics models based on the harmonic approximation—have only started to be used in this field. We describe a 2D solute-segregation induced structural transition in a $\Sigma = 5/(002)$ twist boundary, observed via realistic MC simulations, for a bulk single-phase Pt(Ni) bicrystal at 850 K; this transition has the characteristics of a congruent phase transition.

In addition to the conventional state variables—temperature (T), pressure (P), and bulk composition—the phase space of GB structure is known to include five macroscopic geometrical degrees of freedom (DOF), responsible for the misorientation (c_1, c_2, θ) and interface plane of the two grains (n_1, n_2) [2,3]. Phase transitions for which the five macroscopic state variables do not change are denoted congruent [2,3]. For a congruent phase transition at a GB in a binary alloy, the generalized Clausius-Clapeyron equation is [4]

$$\Delta s_{\mathrm{GB}} dT - \Delta v_{\mathrm{GB}} dP + \Delta\Gamma d\mu = 0\,, \qquad (1)$$

where Δs_{GB}, Δv_{GB}, and $\Delta\Gamma$ are discontinuities in the excess entropy, excess volume, and Gibbsian excess of solute, respectively, of a GB, and μ is the chemical potential of the solute. Since a GB in equilibrium with the bulk crystal is an open thermodynamic system, the bulk concentration affects the phase transition locus in T-P-μ space [Eq. (1)].

One type of congruent phase transition is associated with a change in the microscopic DOFs [3]. Three of the microscopic DOFs are given by the rigid-body translation vector, **p**, between two grains. It is convenient to use only the components of **p** lying in the interfacial plane [5], and it is sufficient to use **p** vectors lying within one GB repeat cell because of the periodicity of the GB structure. For twist boundaries the crystallographically nonequivalent **p** vectors are limited to the cell bordered by the two shortest displacement shift complete (DSC) vectors $\mathbf{b}_1$ and $\mathbf{b}_2$ in the interface plane [Fig. 1(a)]. For a given GB at fixed values of T, P, and the macroscopic geometrical DOF, among the continuum of possible **p** vectors, there may be more than one that correspond to minima of the dependence of the interfacial free energy (γ) on **p**. In most cases these minima coincide with GB structures of high symmetry. The best studied example is the $\Sigma = 5/(002)$ symmetrical twist GB in fcc metals [6], which has been investigated via lattice statics at 0 K for Cu, Ni, and Au [7]. The global minimum of γ is for the coincident site lattice (CSL) structure, Fig. 1(a), with the holosymmetric space

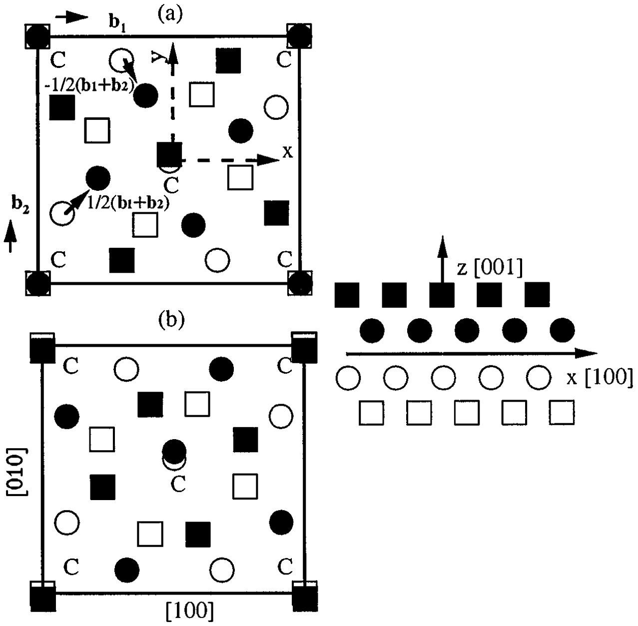

FIG. 1. The (a) CSL and (b) type 2 structures of the $\Sigma = 5/(002)$ twist boundary. The open and solid circles indicate planes -1 and 1, respectively, and the open and solid squares planes -2 and 2. In the CSL structure a solid circle and an open square are in coincidence, while in the type 2 structure it is the two circles and two squares that are in coincidence. The letter *C* indicates overlapping pairs of coincidence sites.

0031-9007/96/77(16)/3379(4)$10.00

group $p42_1'2'$. The fourfold rotational axes are parallel to $\langle 001 \rangle$, and both the twofold rotational ($2'$) and twofold screw ($2_1'$) axes lie in the interfacial plane [8]. A translation by a $\mathbf{b}_1/2$ vector, $\mathbf{b}_1 = (1/10)[130]$, transforms this structure into the type 1 structure with $p22_1'2'$ symmetry. Alternatively, a translation by a $(1/2)(\mathbf{b}_1 + \mathbf{b}_2)$ vector, $\mathbf{b}_2 = (1/10)[310]$, from the CSL structure leads to the type 2 structure [Fig. 1(b)] with the space group $p42'2'$. The type 1 and type 2 structures are found to be metastable with respect to the CSL structure, with γ's at 0 K only several percent higher than that of the CSL structure [7]. The $\Sigma = 5/(002)$ GB in Au has been studied experimentally by x-ray diffraction at room temperature and has a CSL structure [9]. The CSL structure is the one most commonly observed experimentally for elemental fcc metals [5]. Recent simulations point to the possibility of a congruent structural phase transition in the $\Sigma = 5/(002)$ GB of gold at an elevated T [10]. Congruent GB phase transitions induced by solute segregation have only been experimentally observed [11–14].

For simulations we employ the MC method in the transmutational ensemble [15–17]. During a simulation T, the total number of particles, and the difference in the excess chemical potentials, between solute and solvent species, are held constant. The total volume of the computational cell is allowed to relax, resulting in a constant P ensemble. The chemical identities of particles are changed, so that the atomic fraction of each component is a variable. The chemical composition in the reference bulk region is thus constant, while near the interfaces it achieves its equilibrium value. The total internal energy is calculated using embedded atom method (EAM) potentials [18,19]. The computational cell has 3D periodic boundary conditions and contains two grains rotated around a common [001] direction by the twist angle, $\theta = 36.9°$. Because of the periodic boundary conditions, there are two crystallographically identical, but physically different GBs in a bicrystal with a separation of 16 (002) planes. This value is sufficient to avoid elastic interactions between the GBs and to provide a region of unstressed perfect crystal in the middle of each grain. In the plane of the interface the computational cell is approximately 5 nm by 3.8 nm; each (002) plane contains 240 atoms and therefore a bicrystal has 7680 atoms. The first 2.5×10^3 MC steps atom^{-1} are used for equilibration, and the averaging is performed for the next 3×10^3 or 10^4 MC steps atom^{-1}. The time step for averaging is 10 MC steps atom^{-1} to avoid temporal correlation effects. The averaging is performed over the coordinates of each atom i, and this average is identified with the position of an atomic site i. To avoid the effects of γ—which may be considerable in a small computational system—we fix the dimensions of the computational cell in the plane of the interface at the appropriate value for a given T and bulk solute concentration. The periodic length in the direction normal to the interface is allowed to relax to relieve bulk stresses. Rigid-body translations of the two grains, by small random vectors lying in the plane of the interface, are introduced at large intervals of time (in MC steps). This allows efficient relaxation of the microscopic DOFs, i.e., $\mathbf{p}$.

We have performed simulations at bulk solute concentrations of 0.6, 1.0, 1.2, 2.3, 3.0, 5.6, 7, and 12 at. % Ni. The concentrations between 0.6 and 7 at. % Ni exhibit random rigid-body translations in the interface plane with a magnitude between 0.01 and 0.02 nm, as well as a considerable amount of structural disorder at the GB. This implies that the average structure is, in fact, a superposition of many translational states, none of which is preferred. For 0.6, 7, and 12 at. % Ni reproducible well-defined interface structures are observed. We present results for the 0.6 and 7 at. % Ni alloys. First, the concentration profiles normal to the interface are exhibited in Fig. 2. Each data point corresponds to the average solute concentration in one (002) plane parallel to the interface. Because of the periodic boundary conditions there are two crystallographically identical interfaces; i.e., between planes -1 and 1, and -16 and 16, where the negative and positive numbers denote two different grains. The strongest segregation occurs at the first planes immediately adjacent to the interface, and, to a smaller extent, in the second planes. For 0.6 at. % Ni the structure of the four (002) planes adjacent to the GB (two on each side of the interface plane) is exhibited in Fig. 3(a). Note that it retains the CSL structure; compare the outlined unit cell in Fig. 3(a) with Fig. 1(a). Also note that the coincidence sites in the first planes immediately adjacent to the interface (open and solid circles) correspond to the coincident sites [20] in the second plane on the other side of the interface (open and solid squares). The positioning of the two grains with respect to each other is illustrated in Fig. 3(b). The arrangement is the same as in

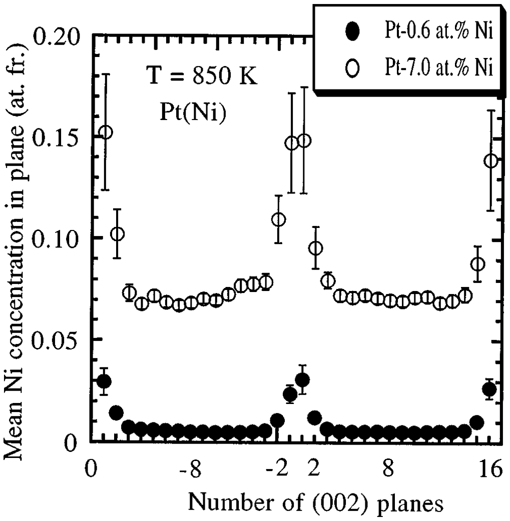

FIG. 2. Concentration profiles of Ni normal to the $\Sigma = 5(002)$ interface in the computational system. The solid circles refer to Pt–0.6 at. % Ni and the open circles to Pt–7 at. % Ni. Because periodic boundary conditions are employed two interfaces are present in this figure; one is between planes -1 and 1, and the second one is between planes -16 and 16.

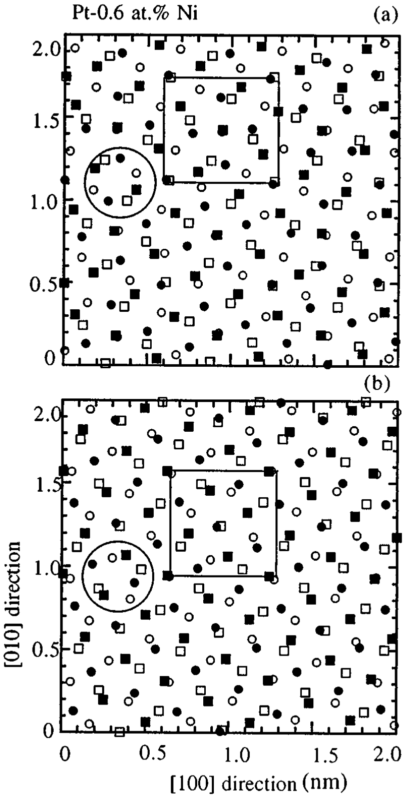

FIG. 3. (a) A portion of the GB structure for Pt–0.6 at.% Ni. The notation is the same as in Fig. 1. (b) The relative position of two adjacent grains by projecting two (002) planes from the bulk of each of the grains onto the interface plane. The stacking sequence is the same as in (a). GB unit cells are indicates in both (a) and (b): compare with Fig. 1(a). Note that in both cases the CSL structure is preserved.

Fig. 3(a), but the (002) planes nearest the GB are substituted by planes from the bulk in the same stacking sequence; i.e., planes $-8, -9, 8, 9$ are substituted for planes -2, -1, 1 and 2. This is also the CSL structure, and no rigid-body translations are present. A different situation is seen in Figs. 4(a) and 4(b) with Fig. 1(b). It is still a $\Sigma = 5$ boundary, but due to the rigid-body translation of the two grains, the coincidence sites in the first planes immediately adjacent to the interface (-1 and 1) are now on top of each other, as well as the coincidence sites in the two second planes (-2 and 2). The average solute concentrations for different GB sites are given in Table I for the 0.6 and 7 at.% Ni alloys, which demonstrates that for 0.6 at.% Ni, strong solute-atom enhancement occurs at the noncoincident sites in both planes, while the coincidence sites are slightly depleted in solute. Conversely, for 7 at.% Ni the highest enhancement occurs for the coincident sites, while the noncoincident sites exhibit a significantly smaller enhancement.

Next we demonstrate that there is a local chemical ordering at the interface. Ordering implies strong correlations in the chemical occupancies of neighboring atomic sites; i.e., atoms of different species have a significantly higher probability of being neighbors than such a probability calculated from a random solid-solution model. Such an ordering is found only in pairs of adjacent coincidence sites in the type 2 structure. These sites are located across the plane of the interface from each other in the planes ± 1 as shown in Fig. 1(b). We denote the Ni concentrations at these sites c_i^1 and c_i^{-1}, where the subscript identifies a pair of the sites and the superscript identifies the plane in which a site is located. Both $\langle c_i^1 \rangle$ and $\langle c_i^{-1} \rangle$ are equal to ≈ 43 at.%, but the distributions are unusually broad and flat. The distribution, however, of $(c_i^1 + c_i^{-1})/2$ is sharply peaked at ≈ 43 at.%. Moreover, within statistical error a linear relation is observed, $c_i^1 = 0.86 - c_i^{-1}$. This points to a strong correlation between c_i^1 and c_i^{-1}. It is not surprising that we observe local ordering at this boundary as the Ni-Pt system exhibits bulk ordering at 850 K at higher concentrations.

In summary, we have observed a congruent or 2D structural GB phase transition at a $\Sigma = 5/(002)$ twist boundary induced by solute segregation for a single-phase Pt(Ni) bicrystal at 850 K. This GB transition occurs at solute concentrations when the bulk is definitely in a single-phase solid-solution region. Below the phase transition point in the bulk Ni concentration (0.6 at.% Ni) the equilibrium structure is the CSL structure. At 7 at.% Ni (bulk value) the type 2 structure is detected; it is obtained from the CSL structure via a $(1/2)(\mathbf{b}_1 + \mathbf{b}_2)$

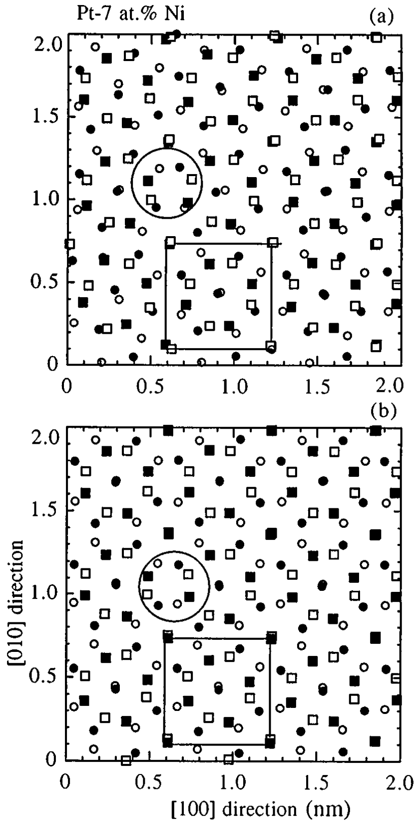

FIG. 4. The same information is displayed as in Fig. 3, but for Pt–7 at.% Ni. Note that both (a) and (b) have a type 2 structure. GB unit cells are indicated in both (a) and (b): compare with Fig. 1(b).

TABLE I. Average concentrations of Ni at different GB sites in the CSL and type 2 structures for Pt–0.6 at.% Ni and Pt–7.0 at.% Ni alloys at 850 K for the $\Sigma = 5/(002)$ twist boundary.

Bulk Ni concentration	Coincident sites in planes ±1	Noncoincident sites in planes ±1	Coincident sites in planes ±2	Noncoincident sites in planes ±2
0.60 at.%	0.26	3.44	0.90	1.34
7.00 at.%	43.30	7.09	13.30	9.60

rigid-body translation. We have also observed small rigid-body translations and considerable structural and chemical disordering in the same GB at 3 at.% Ni (bulk value) [21] due to the superposition of different translational states. The fact that the transition region is so wide may have two explanations: (a) The presence of a two-phase region in concentration, where the two phases coexist—such a region would not appear in this simulation because in the Monte Carlo procedure the two grains are displaced as a whole during the run. (b) In Monte Carlo simulations the phase transition point can be considerably smeared out in a small computational system [1,22]. Both explanations may be true simultaneously. Explanation (b) is difficult to verify, because an unrealistic increase in the size of the simulation cell is needed to narrow significantly the transition region. The presence of a two-phase region can be investigated, e.g., via simulations. The question of the order of the phase transition remains open. Most probably it is a first order, with a metastable phase becoming stable at some solute concentration. A second-order transition is more difficult to imagine in this situation, but it cannot be ruled out. For a definite answer thermodynamic data are required that can, with some effort, be obtained from MC simulations. Most importantly, GB phases differing by the value of **p** can be investigated experimentally [23]. Finally, our unpublished results indicate that the Ni-rich side of the bulk phase diagram a phase transition does not occur. It is emphasized that not only is the phase transition induced by solute segregation, but the pattern of segregation at different GB sites is different. This suggests chemical ordering at the GB, while the bulk is chemically disordered [24]. A mean-field theory with a rigid atomic structure cannot predict this transformation [25].

We thank A. Z. Patashinskii and J. D. Rittner for helpful discussions. This research is supported by the NSF (Grant No. DMR-9419171) and is partially supported by Grant No. DMR920002N at the NCSA at the University of Illinois at Urbana-Champaign. This work made use of MRL Central facilities supported by the NSF, at the Materials Research Center of Northwestern University, under DMR-9120521.

[1] C. Rottman, J. Phys. (Paris), Colloq. **49**, C5-313 (1988).
[2] J. W. Cahn, J. Phys. (Paris), Colloq. **43**, C6-192 (1982).
[3] A. P. Sutton and R. W. Balluffi, *Interfaces in Crystalline Solids* (Oxford University Press, New York, 1995), p. 405.
[4] E. W. Hart, in *The Nature and Behavior of Grain Boundaries*, edited by H. Hu (Plenum Press, New York, 1972), p. 185.
[5] D. N. Seidman, in *Materials Interfaces: Atomic-Level Structure and Properties,* edited by D. Wolf and S. Yip (Chapman & Hall, London, 1992), p. 58.
[6] Σ is the ratio of the volume of the unit cell of the CSL to the volume of the unit cell in direct lattice space.
[7] D. Schwartz *et al.,* Acta Metall. **36**, 675 (1988).
[8] R. C. Pond and W. Bollmann, Philos. Trans. R. Soc. London A **292**, 449 (1979).
[9] M. R. Fitzsimmons and S. L. Sass, Acta Metall. **36**, 3103 (1988); **37**, 1009 (1989); I. Majid *et al.,* Phys. Rev. B **40**, 2779 (1989).
[10] R. Najafabadi, D. J. Srolovitz, and R. LeSar, J. Mater. Res. **5**, 2663 (1990); J. Mater. Res. **6**, 999 (1991).
[11] R. Herschitz and D. N. Seidman, Acta Metall. **33**, 1547, 1565 (1985).
[12] K. Sickafus and S. L. Sass, Acta Metall. **35**, 69 (1987).
[13] D. E. Luzzi, M. Yan, M. Sob, and V. Vitek, Phys. Rev. Lett. **67**, 1894 (1991).
[14] A. Charai and J. L. Rouviere, Mater. Res. Soc. Symp. Proc. **319**, 417 (1994).
[15] S. M. Foiles, in *Surface Segregation and Related Phenomena,* edited by P. A. Dowben and A. Miller (CRC Press, Boca Raton, Florida, 1990), p. 79.
[16] S. M. Foiles, Phys. Rev. B **40**, 11 502 (1989).
[17] A. Seki *et al.,* Acta Metall. Mater. **39**, 3167 (1991); **39**, 3179 (1991); D. Udler and D. N. Seidman, Phys. Status Solidi (b) **172**, 267 (1992); Acta Metall. Mater. **42**, 1959 (1994).
[18] M. S. Daw and M. I. Baskes, Phys. Rev. Lett. **50**, 1285 (1983); Phys. Rev. B **29**, 6443 (1984).
[19] S. M. Foiles, M. I. Baskes, and M. S. Daw, Phys. Rev. B **33**, 7983 (1986).
[20] Coincidence is used here in a 2D sense, i.e., sites are coincident when their projections onto the planes of the interface coincide. This is distinct from coincidence in the CSL, which is a 3D construction.
[21] D. Udler and D. N. Seidman, Interface Sci. **3**, 41 (1995).
[22] M. P. Allen and D. J. Tildesley, *Computer Simulation of Liquids* (Clarendon Press, Oxford, England, 1987), pp. 25, 26.
[23] C. P. Sun and R. W. Balluffi, Philos. Mag. **46**, 49 (1982).
[24] Similar phenomena were observed experimentally in stacking faults in dilute single-phase Co(Nb) and Co(Fe) alloys via atom-probe microscopy: see Ref. [11].
[25] A. Brokman, Acta Metall. **35**, 307 (1987).